

MOISTURE DISTRIBUTION, DIFFUSION COEFFICIENT, AND SHRINKAGE OF
CEMENT-BASED MATERIALS

(Translation from Proceedings of JSCE, No.634/V-45, November 1999)



Toshiki AYANO



Kenji SAKATA



Folker H. WITTMANN

The aim of this study was to develop a new method to determine hygral diffusion, film, and shrinkage coefficients of cement-based materials. These coefficients are required in the numerical simulation of shrinkage strain and total deformation of concrete elements and structures using the finite element method. Both an experimental approach to determine the time-dependent distribution of relative humidity distribution in the pore system of concrete and a numerical method to determine material coefficients on the basis of experimental data are described in this paper. The hygral diffusion coefficient can be expressed both as function of moisture content and as function of relative humidity.

Key Words: diffusion coefficient, relative humidity distribution, drying shrinkage strain, inverse analysis, sliced specimen

T. Ayano, associate professor in environmental and civil engineering at Okayama University, Okayama, Japan, received his Doctor of Engineering degree from Okayama University in 1993. His research interests include prediction of concrete shrinkage and creep. He is a member of the JSCE.

K. Sakata, professor in environmental and civil engineering at Okayama University, Okayama, Japan, received his Doctor of Engineering degree from Kyoto University, Japan in 1976. His research interests include prediction of concrete shrinkage, creep, and fatigue properties. He is a fellow of the JSCE.

F. H. Wittmann, professor in the Institute for Building Materials at the Swiss Federal Institute of Technology, Zurich, Switzerland, received a "Dr. rer. nat." degree from University of Technology in Munich in 1965 and honore doctorate in engineering from University Essen, Germany in 1998. His research interests include fracture mechanics, creep, shrinkage, material science, material chemistry, and durability.

1. INTRODUCTION

Shrinkage strain develops as moisture is lost from cement-based materials such as concrete. Such strain therefore develops much quicker near the drying surface than in the center of concrete. If a concrete member were to consist of separate unrestrained elements of infinitesimal thickness, the relationship between change in moisture content and deformation would be linear [1]. In a real concrete member, however, the strain due to quicker drying near the surface as compared to the inside of the concrete produces tensile and compressive elastic strains due to eigenstresses. In order to simulate numerically the effect of drying on the deformation of concrete, the diffusion, film, and shrinkage coefficients are required. By using the diffusion and film coefficients together, the moisture distribution at any arbitrary time during drying can be obtained. The unrestrained drying shrinkage strain is calculated by multiplying the change in moisture content by the shrinkage coefficient. Finally, the deformation can be calculated according to the principle of virtual work.

The diffusion coefficient of concrete is nonlinear and depends on the moisture content itself. If the diffusion coefficient can be expressed in terms of the relative humidity in the concrete, the analysis of drying is exactly the same as that for the thermal case. The ambient relative humidity can be used as the boundary condition in a numerical analysis.

To obtain the nonlinear diffusion coefficient, various methods have been proposed by different researchers [2][3]. However, all are for the nonlinear diffusion coefficient in terms of moisture content rather than in terms of relative humidity. To determine the diffusion coefficient as a function of the pore equilibrium relative humidity of the concrete, the relationship between moisture content at hygral equilibrium and the relative humidity, i. e. the desorption isotherm (which varies with ambient temperature) must be known. Experimentally derived desorption isotherms are available for some cement-based materials. However, it is not clear whether they are suitable for any concrete. Furthermore, it takes a lot of time to determine a desorption isotherm by experiment. A method of obtaining the diffusion coefficient as a function of relative humidity directly by experiment is desirable.

A useful and reliable method of obtaining a diffusion coefficient as a function of relative humidity is proposed in this paper. An experiment is carried out with sliced specimen measuring 150x100x3 mm. Each specimen is prepared by piling up 11 slices and sealing the sides with aluminium sheet. The distribution of relative humidity is estimated by measuring the shrinkage strain on each slice at arbitrary drying times. An inverse analysis is then used to obtain the diffusion coefficient from the measured relative humidity distribution. A numerical approach based on the weighted residual method and on a nonlinear least squares method is then proposed on the basis of the experimental results.

2. OUTLINE OF THE EXPERIMENT

2.1 Mix proportions of mortar and concrete

In this research, normal Portland cement type-I (specific gravity: 3.12) was used. The fine aggregate was river sand (specific gravity: 2.62; water absorption: 1.93%). The coarse aggregate was river gravel (maximum size: 8 mm and 16 mm; specific gravity: 2.70; water absorption: 0.62%). Mix proportions of mortar and concrete are shown in **Table 1**. The mechanical properties of the mortar and concrete are shown in **Table 2**. These data were obtained at ages of 14 days and 120 days. Two types of specimen were used for strength tests at the age of 120 days. One was cured in water for 120 days, the other was cured in water for 14 days and then in air for a further 106 days.

Table 3 shows the physical properties of the mortars and concretes studied. The evaporable moisture content was obtained using eight slices measuring 150x100x3 mm. The specimens were dried at 100 C for 14 days after curing in water for 7 days and subsequently in a chamber at 100% relative humidity for 7 days. All sliced specimens used in this study (150x100x3 mm) were sawed from cubes (150x150x150 mm). Carbonated thickness was measured using phenolphthalein. The specimens for carbonation test were cured in water for 14 days and subsequently in air for 98 days. Three rooms of 45%, 60%, and 75% relative humidity were used. In each room, the temperature was 20 C.

Table 4 shows the moisture loss when mortar and concrete specimens reached equilibrium with the surrounding atmosphere. These data were obtained from the center three slices originally packed in specimens prepared by piling up 11 slices (150x100x3 mm) and sealing the sides with aluminium sheet. The specimens were stored for 98 days at

Table 1 Mix proportions of mortar and concrete

Mixture	G _{max} (mm)	W/C (%)	s/a (%)	Weight per unit volume (kg/m ³)					
				W	C	S	G		*1
							4-8	8-16	
M240	4	50	100	240	480	1536	—	—	—
M200	4	50	100	200	400	1708	—	—	—
M160	4	50	100	156	320	1880	—	—	3.84
G8	8	50	50	200	400	854	880	—	—
G16	16	50	50	200	400	854	352	528	—

*1: Superplasticizer

Table 2 Mechanical properties of mortar and concrete

Mixture	Age (days)	Comp. Strength (MPa)	Young's Modulus (G Pa)	Flexural Strength (MPa)	
M240	14	33.6	25.8	6.16	
	120	Air	44.4	26.3	8.38
		Water	45.4	30.3	8.53
M200	14	32.1	24.8	5.10	
	120	Air	41.5	27.4	7.84
		Water	44.3	29.3	8.33
M160	14	19.2	22.1	4.16	
	120	Air	21.5	19.6	4.61
		Water	29.6	19.4	4.69
G8	14	42.0	31.8	6.74	
	120	Air	48.3	36.7	10.1
		Water	52.8	39.5	10.3
G16	14	36.4	31.6	6.59	
	120	Air	49.7	33.6	8.31
		Water	55.7	38.6	8.98

Table 3 Physical properties of mortar and concrete

Mixture	Evaporable moisture		Density (g/cm ³)	Carbonation (mm)*
	w/(S+w)	w/S		
M240	8.94%	9.82%	2.12	3
M200	7.35%	7.93%	2.15	3
M160	6.59%	7.05%	1.99	10
G8	6.18%	6.59%	2.36	1
G16	6.20%	6.61%	2.32	1

w: evaporable moisture content (g)

S: solid part of mortar or concrete

*: all relative humidities

Table 4 Moisture loss compared with the moisture content under saturated condition (w'/w)

Mixture	Relative humidity		
	45%	60%	75%
M240	69.1%	65.7%	51.7%
M200	68.8%	64.5%	53.0%
M160	77.4%	76.2%	68.4%
G8	62.6%	57.5%	51.9%
G16	64.4%	60.9%	51.5%

w': moisture loss measured at each relative humidity

each relative humidity after curing in water for 7 days and subsequently in a chamber at 100% relative humidity for 7 days. The values shown in this table are normalized with respect to the moisture content under saturated conditions as shown in **Table 3**.

2.2 Geometry of specimens

a) Specimens for moisture distribution

Figure 1 shows the sliced specimen used for the determination of moisture distribution. A pile of sliced specimen consists of 11 slices of the size of 150x100x3 mm. Solid specimens of 150x100x33 mm are also used in this series of experiments. All surfaces, except the two parallel drying surfaces, were sealed with aluminum sheet. Two solid specimens and nine sliced specimens were put into each room with a relative humidity of 45%, 60%, and 75%, respectively. Altogether, 6 solid specimens and 27 sliced specimens were used for each type of mortar and concrete. The temperature of all rooms was 20 C. Drying began at 14 days. The weight of each specimen was measured at 0.5, 1, 2, 3, 5, 7, 10, 14, 21, 28, 35, 42, 56, 70, and 98 days after the start of drying. At 0.5, 3, 7, 14, 28, 42, 56, 70, and 98 days after the start of drying, the aluminum sheet was removed from one sliced specimen in order to obtain the moisture loss of each slice. After the moisture loss was measured, the specimen was discarded.

b) Specimens for shrinkage strain distribution

Figure 2 shows the sliced specimen used for the investigation of shrinkage strain. A pile of sliced specimen consists of 11 slices (150x100x3 mm). **Figure 3** shows the position of the gauge points on the sliced specimens. The gauge

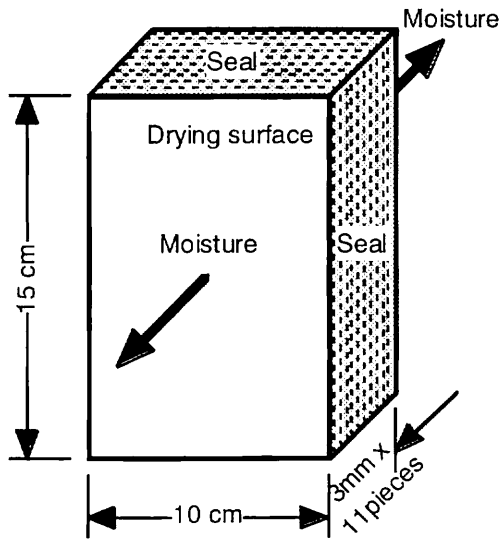


Fig.1 Sliced specimen for measuring moisture loss

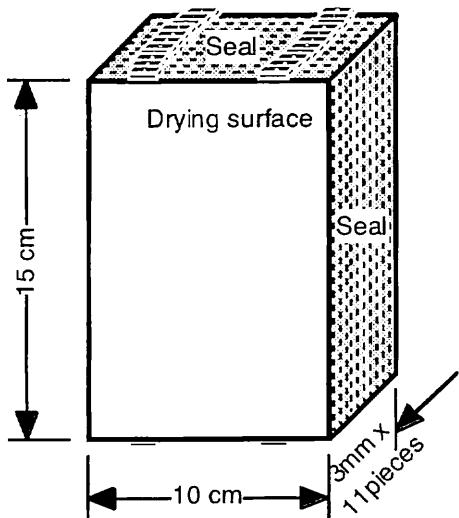


Fig.2 Sliced specimen for measuring shrinkage strains

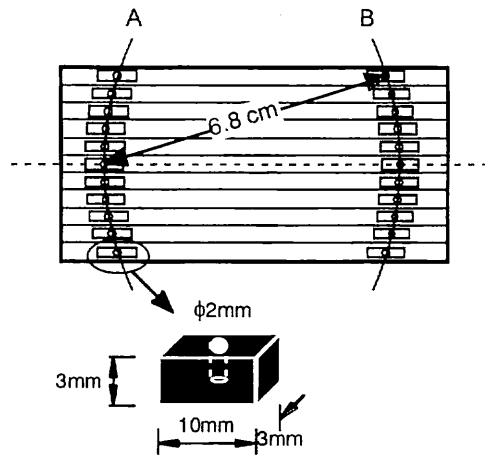


Fig.3 Point gauges on sliced specimens

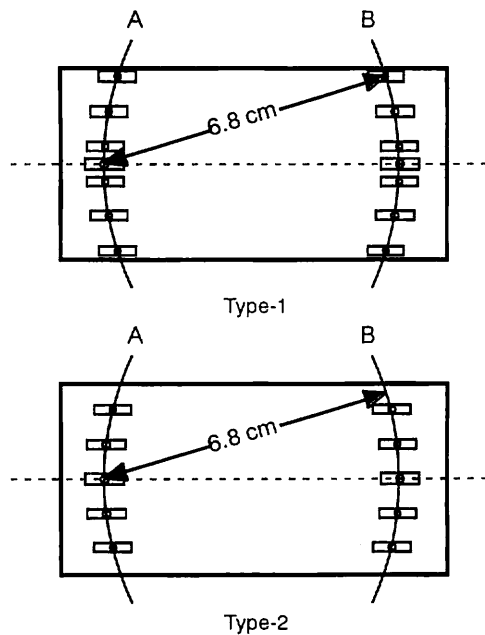


Fig.4 Point gauges on solid specimens

points are located on the top and bottom surfaces in two arcs. Row B is on an arc centered on the gauge on the 6th (middle) layer in row A. The gauge points in row A are similarly centered on the 6th slice of row B. The size of the solid specimens was 150x100x33 mm. **Figure 4** shows the position of gauge points on the solid specimens. There are two types of solid specimen. The difference is the position of the gauge points. The placement of gauge points is the same as in the case of sliced specimens, except that they are placed every second layer. The gauge points are made of 3x3x10 mm brass and have a 2 mm hole. Four surfaces of both types of specimen were sealed with aluminum sheet. The shrinkage strains were measured in the rooms with relative humidities of 45%, 60%, and 75%, respectively. Drying began after the specimens were cured in water for 7 days and subsequently in a chamber at 100% relative humidity for 7 days. The shrinkage strain of each specimen was measured at 0.5, 1, 2, 3, 5, 7, 10, 14, 21, 28, 35, 42, 56, 70, and 98 days after the start of drying.

2.3 Moisture content related to saturation value

The weights of the specimens were measured using an electronic balance with a minimum division of 1/100 g and a capacity of 5,000 g. With the weight $C(t)$ at drying time t and the weight $C'(t)$ after 14 days in an oven, the moisture content $q(t)$ can be obtained from equation (1):

$$q(t) = \frac{w - w'(t)}{S + w - w'(t)} = \frac{C(t) - C'(t)}{C(t)} \quad (1)$$

where, S is the weight of the solid part of the concrete or mortar, i. e. $C'(t)$; $w'(t)$ is the weight of moisture lost; and w is the weight of moisture in the saturated condition. If the moisture content in the saturated condition is called p , then the moisture lost per unit weight of concrete or mortar $H(t)$ can be calculated from equation (2).

$$H(t) = \frac{w'(t)}{S + w} = \frac{p - q(t)}{1 - q(t)} \quad (2)$$

$$p = \frac{w}{S + w} = \frac{C(0) - C'(0)}{C(0)} \quad (3)$$

Where, $C(0)$ is the original weight of the specimen when drying time t is zero; and $C'(0)$ is the weight of the specimen after drying in an oven for 14 days. The moisture content $\omega(t)$ with respect to moisture content in the saturated condition can be obtained from equation (4).

$$\omega(t) = 1 - \frac{w'(t)}{w} = 1 - \frac{1}{p} \times H(t) \quad (4)$$

2.4 Measuring method for shrinkage strain

In **Figure 5**, the procedure for measuring shrinkage strain is illustrated. Length change in the longitudinal direction was measured using a linear gauge with a minimum division of 1/1,000 mm. The specimen was supported on three pins consisting of the pointed head of the linear gauge and two supports. Dividing the change in length by the height of the specimen gives the shrinkage strain. When measuring the shrinkage strain in row A, one of the two supports is placed on the gauge point on the bottom of the sixth slice in row B. The second is placed on the bottom gauge point of the slice to be measured. The tip of the linear gauge is placed on the top of the slice to be measured.

3. MOISTURE DISTRIBUTION

3.1 Effect of gaps in sliced specimens on moisture transfer

The diffusion coefficient of moisture transfer in air is approximately 218 mm²/day at 20 C. This is about 50 or 100 times faster than in mortar or concrete [4]. This means that the transfer of moisture through the air is much easier than through mortar or concrete. However, the air layer between slices may act as an obstacle to moisture transfer in the sliced specimens if the gap is considerable.

Figure 6 shows the weight change of a solid specimen (150x100x33 mm) and a pile of sliced specimen (150x100x3 mm x11slices) for mortar M240 in **Table 1**. The weight change expressed on the vertical axis was obtained by equation (5).

$$\text{Weightchange} = \frac{C(0) - C(t)}{C(0)} \quad (5)$$

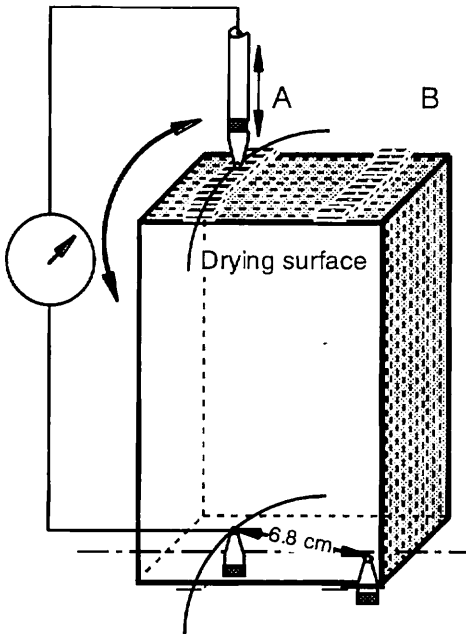


Fig.5 Method of shrinkage strain measurement

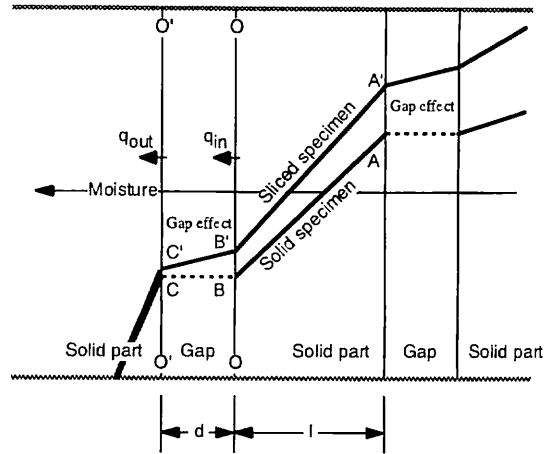


Fig.7 Effect of gaps on moisture transfer

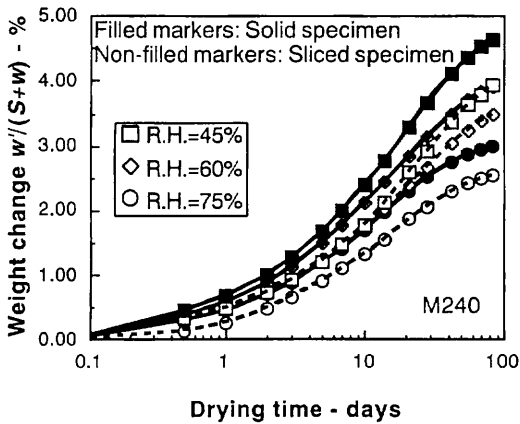


Fig.6 Weight change of solid and sliced specimens

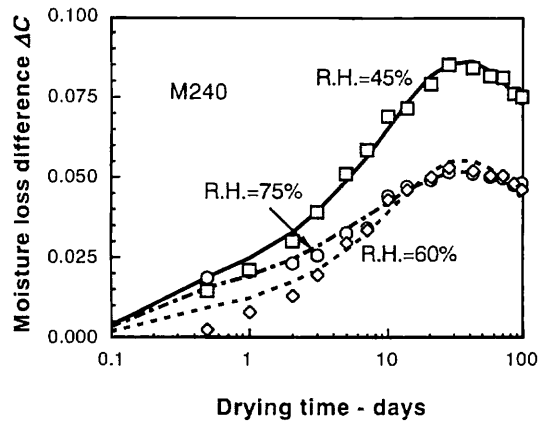


Fig.8 Moisture loss difference

where, $C(0)$ is the weight of specimen when drying time is zero; and $C(t)$ is the weight of the specimen at drying time t . The solid marks represent the data obtained from the solid specimen. The open marks represent the data obtained from the sliced specimen. Squares, lozenges, and circles indicate different relative humidities of 45%, 60%, and 75%, respectively. The results clearly show the solid specimen loses moisture faster than the sliced specimen. This is due to the effect of gaps between slices.

This can be explained using Figure 7. The curves $A'B'C'$ and curve ABC express the assumed moisture distribution in sliced and solid specimens, respectively. When q_{in} and q_{out} are the moisture flows per unit time from surface $O-O$ into an air gap and from an air gap into surface $O'-O'$, respectively, q_{out} minus q_{in} is equal to the moisture change in the gap formed by OO and $O'O'$.

$$q_{out} - q_{in} = \frac{1}{2} \frac{\partial(\omega_B + \omega_{C'})}{\partial t} \times d \quad (6)$$

where, ω_B and ω_C are moisture contents at the position B' and C', respectively; and d is the thickness of the gap between slices. If the gap has zero thickness, q_{out} must be equal to q_{in} ; that is, the moisture contents at surfaces O-O and O'-O' are the same. Whereas, when d cannot be ignored, the slope of moisture increases in the gap. With the slope of moisture in the gap and the diffusion coefficient D_{air} of air, the moisture flow q_{out} can be expressed by equation (7).

$$q_{out} = D_{air} \frac{\omega_{B'} - \omega_{C'}}{d} = q_{in} + \frac{1}{2} \frac{\partial(\omega_{B'} + \omega_{C'})}{\partial x} \times d \quad (7)$$

Since q_{out} is bigger than q_{in} , $\omega_{B'}$ must be bigger than $\omega_{C'}$. The wider the gap d , the bigger the difference between $\omega_{B'}$ and $\omega_{C'}$. Hence, the sliced specimen loses its moisture slower than the solid specimen (Q. E. D.).

Figure 8 shows the difference in moisture loss between the sliced and solid specimens. Squares, lozenges, and circles represent results at 45%, 60%, and 75% relative humidity, respectively. The difference in moisture loss is related to the saturated moisture content; equation (8).

$$\text{Moisture loss difference } \Delta C = \frac{1}{p} \times (\Delta C_{solid}(t) - \Delta C_{sliced}(t)) \quad (8)$$

$$\Delta C_{sliced}(t) = \frac{C_{sliced}(0) - C_{sliced}(t)}{C_{sliced}(0)} \quad (9)$$

$$\Delta C_{solid}(t) = \frac{C_{solid}(0) - C_{solid}(t)}{C_{solid}(0)} \quad (10)$$

where, p is the moisture content normalized with respect to the weight of the specimen under saturated conditions and expressed by equation (3); $C_{sliced}(t)$ and $C_{solid}(t)$ are the weight of sliced and solid specimens at arbitrary drying time t , respectively; and $C_{sliced}(0)$ and $C_{solid}(0)$ are the weight of sliced and solid specimens when drying time is zero. The moisture loss difference shown in **Figure 8** is due to the moisture transport disturbed by air gaps. The moisture loss difference has a peak and finally disappears, as shown in **Figure 8**.

In this study, the moisture distribution obtained from a pile of sliced specimen is used as a substitute for that of the solid specimen in order to obtain the diffusion coefficients. If the effect of gaps is ignored or the thickness of gaps is regarded as zero, then the moisture distribution in **Figure 7** decreases from A'B'C' to ABC. Before this substitution is applied, it has to be confirmed that the effect of gaps on the moisture flow in a pile of sliced specimen is small or negligible.

3.2 Moisture loss distribution

If the moisture loss of a pile of sliced specimen $g(x)$ at position x is represented by a power expression, then equation (11) can be derived.

$$g(x) = a(x_{center} - x)^n + c \quad (11)$$

$$x_{center} = 16.5 \text{ mm} \quad (12)$$

where, $x(mm)$ is the distance from the drying surface; and a , n , and c are constants determined from experimental data. Equations (11) and (12) describe the zero gradient of moisture loss at the center of a specimen due to the symmetrical boundary condition. When $g(x)$ is the moisture loss per unit cross section, the total moisture loss of sliced specimen Q_{sliced} can be expressed by equation (13).

$$\begin{aligned} \frac{1}{2A} \times Q_{sliced} &= \int_{x_{surface}}^{x_{center}} g(x) dx \\ &= \frac{a}{n+1} x_{center}^{n+1} + x_{center} \times c = \sum_{i=1}^6 l_i \times g_i \end{aligned} \quad (13)$$

where, $A(=100 \times 150 \text{ mm}^2)$ is the drying surface; and l_i is the thickness of the slice. The surface slice is $i=1$. The center slice is $i=6$. That is, $l_i=3 \text{ mm}$ when $i=1$ to 5 ; $l_6=1.5 \text{ mm}$ due to the symmetrical boundary condition, and g_i is the moisture loss of each slice. The moisture loss of the surface slice and center slice can be represented approximately by equations (14) and (15), respectively.

$$g(x_{surface} = 0) = a \times x_{center}^n + c = \frac{g_1 - g_2}{3} \times 1.5 + g_1 \quad (14)$$

$$g(x_{center}) = c = g_6 \quad (15)$$

The constant c involved in $g(x)$ can be obtained by equation (15). From equations (13) and (14), equation (16) is derived for constant n . Constant a can be determined by equation (17).

$$n = \frac{\left(\frac{g_1 - g_2}{3} \times 1.5 + g_1 - g_6 \right) \times x_{center}}{\sum_{i=1}^6 l_i \times g_i - x_{center} \times g_6} - 1 \quad (16)$$

$$a = \frac{g(x_{surface}) - g_6}{x_{center}^n} \quad (17)$$

When $f(x)$ is the moisture loss within a solid specimen, the total moisture loss of solid specimens Q_{solid} can be expressed by equation (18).

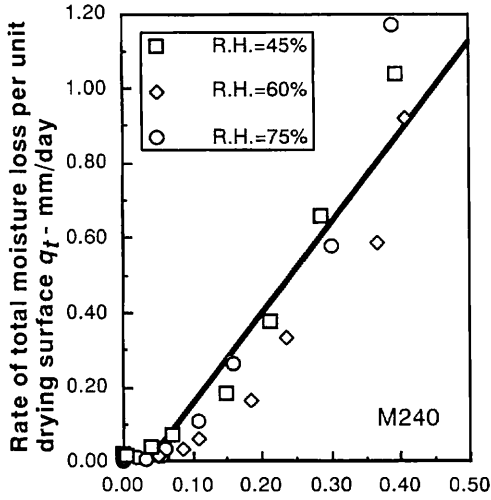
$$\frac{1}{2A} \times Q_{solid} = \int_{x_{surface}}^{x_{center}} f(x) dx = \sum_{i=1}^6 l_i \times g_i + \frac{L}{2} \times \Delta C \quad (18)$$

where, ΔC is the moisture loss difference between a solid specimen and a pile of sliced specimen, as shown in **Figure 8**. L is the thickness of the specimen, i. e. 33 mm . The moisture loss at the drying surface of a solid specimen $f(x_{surface})$ can be determined from the moisture loss of the surface layer of a pile of sliced specimen $g(x_{surface})$ and the moisture loss difference on the drying surfaces between solid and sliced specimens Δh_s . Δh_s is calculated from the film coefficient H_F and $d\Delta C/dt$ as follows.

$$\begin{aligned} \Delta h_s &= \frac{1}{H_F} \times \frac{1}{2A} \times \left(\frac{dQ_{solid}}{dt} - \frac{dQ_{sliced}}{dt} \right) \\ &= \frac{1}{H_F} \times \frac{L}{2} \times \frac{d\Delta C}{dt} \end{aligned} \quad (19)$$

$d\Delta C/dt$ is the ratio of moisture loss difference between a solid specimen and a pile of sliced specimen. Δh_s is zero when $d\Delta C/dt$ is equal to zero. Δh_s remains zero and can never become negative because the ratio of moisture loss of a pile of sliced specimen is never greater than that of a solid specimen. Equation (19) is derived from equations (20) and (21).

$$\frac{1}{2A} \times \frac{dQ_{sliced}}{dt} = H_F \left(g(x_{surface} t_{\infty}) - g(x_{surface} t) \right) \quad (20)$$



Moisture loss differential at ultimate and arbitrary times ($\omega_{surface} - \omega_a$)

Fig.9 Relationship between q_t and $\omega_a - \omega_{surface}$

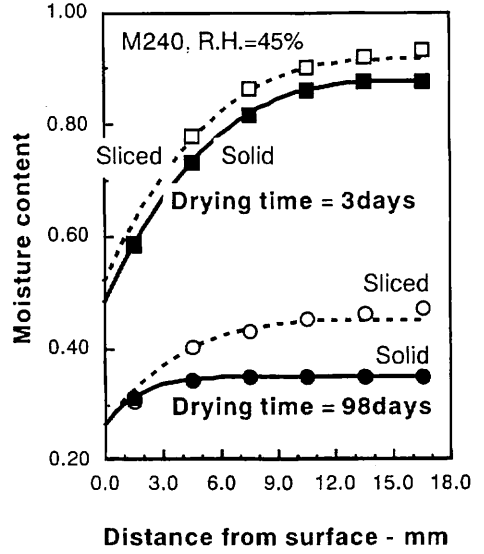


Fig.10 Moisture distribution of each specimen

$$\frac{1}{2A} \times \frac{dQ_{solid}}{dt} = H_F (f(x_{surface}, t_{\infty}) - f(x_{surface}, t)) \quad (21)$$

where, $g(x_{surface}, t_{\infty})$ and $f(x_{surface}, t_{\infty})$ are the moisture loss of the surface layer of sliced and solid specimens at the ultimate drying time, respectively. These two values must be the same. The film coefficient H_F expresses the relationship between q_t and $\omega_{surface} - \omega_a$, where q_t is the moisture that passes through a unit area of the drying surface per unit time. $\omega_{surface}$ is the moisture loss through the drying surface at an arbitrary drying time. ω_a is the moisture loss when the relative humidity of the cement-based material is equal to that of the surrounding atmosphere.

$$q_t = H_F \times (\omega_a - \omega_{surface}) = \frac{1}{2A} \times \frac{dQ_{sliced}}{dt} \quad (22)$$

Figure 9 shows the relationship between q_t and $\omega_{surface} - \omega_a$ for the sliced specimens. It is independent of the ambient relative humidity. The film coefficient of this material is 2.43 mm/day.

When $f(x)$ is expressed by equation (23), the moisture loss through the drying surface of the solid specimen can be expressed by equation (24).

$$f(x) = \alpha (x_{center} - x)^{\beta} + \gamma \quad (23)$$

$$f(x_{surface}) = \alpha \times x_{center}^{\beta} + \gamma = g(x_{surface}) + \Delta t_s \quad (24)$$

Both the moisture content and the moisture distribution gradient in solid specimens are smaller than those of sliced specimens because the moisture transfer in sliced specimens is disturbed by air gaps. If the gradients of moisture distribution at the drying surfaces of sliced and solid specimens are considered equal, the following equation can be derived. Under this hypothesis, the difference in moisture content at the center of each specimen is a maximum.

$$\frac{df(x_{surface})}{dx} = \alpha \times \beta \times x_{center}^{\beta-1} = \frac{dg(x_{surface})}{dx} \quad (25)$$

By using equations (18), (24), and (25), constants α , β , and γ can be obtained as follows.

$$\beta = \frac{x_{center}^2 \times \frac{dg(x_{surface})}{dx}}{(g(x_{surface}) + \Delta h_s) \times x_{center} - \sum_{i=1}^6 l_i \times g_i - \frac{L}{2} \times \Delta C} - 1 \quad (26)$$

$$\alpha = \frac{\frac{dg(x_{surface})}{dx}}{\beta \times x_{center}^{\beta-1}} \quad (27)$$

$$\gamma = g(x_{surface}) + \Delta h_s - \alpha \times x_{center}^{\beta} \quad (28)$$

Figure 10 shows the moisture distribution of sliced and solid specimens. The moisture loss shown in this figure is normalized with respect to the moisture content under saturated conditions. The drying times are 3 days and 98 days. Open circles and squares are the experimental results obtained from sliced specimens. The solid circles and squares are the moisture distributions of solid specimens estimated using equation (23). It is evident that the moisture distribution in sliced specimens can be represented by a power expression. From this comparison of the moisture distributions of sliced and solid specimens, it is confirmed that the effect of the gap between slices seems to be small.

3.3 Diffusion coefficient as a function of moisture content

Equation (29) is the diffusion equation in one dimension.

$$\frac{\partial \omega(x,t)}{\partial t} = \frac{\partial}{\partial x} \left(D(\omega) \times \frac{\partial \omega(x,t)}{\partial x} \right) \quad (29)$$

where, $\omega(x,t)$ is the moisture content; $D(\omega)$ is the diffusion coefficient which is a function of moisture content $\omega(x,t)$; and x and t are distance in the direction of specimen thickness and drying time, respectively. Equation (29) must be satisfied everywhere in the specimen. Equation (30) holds with respect to an arbitrary function $F(x,t)$.

$$\int_{x_{surface}}^{x_{center}} F(x,t) \left\{ \frac{\partial}{\partial x} \left(D(\omega) \times \frac{\partial \omega(x,t)}{\partial x} \right) - \frac{\partial \omega(x,t)}{\partial t} \right\} dx = 0 \quad (30)$$

By means of partial integration, the first term of equation (30) is rewritten as follows.

$$\begin{aligned} & \int_{x_{surface}}^{x_{center}} F \times \frac{\partial}{\partial x} \left(D \times \frac{\partial \omega}{\partial x} \right) dx \\ &= \left[F \times D \times \frac{\partial \omega}{\partial x} \right]_{x_{surface}}^{x_{center}} - \int_{x_{surface}}^{x_{center}} \frac{\partial F}{\partial x} \times D \times \frac{\partial \omega}{\partial x} dx \end{aligned} \quad (31)$$

Substituting equation (31) into equation (30) leads to equation (32).

$$\begin{aligned} & \int_{x_{surface}}^{x_{center}} D \times \frac{\partial F}{\partial x} \times \frac{\partial \omega}{\partial x} dx \\ &= \left[F \times D \times \frac{\partial \omega}{\partial x} \right]_{x_{surface}}^{x_{center}} - \int_{x_{surface}}^{x_{center}} F \times \frac{\partial \omega}{\partial x} dx \end{aligned} \quad (32)$$

From the boundary conditions, equations (33) and (34) are derived.

$$q_t = -D \times \frac{\partial \omega(x_{surface}, t)}{\partial x} \quad (33)$$

$$\frac{\partial \omega(x_{center}, t)}{\partial x} = 0 \quad (34)$$

where, q_t is the moisture content which passes through a unit drying surface area per unit time. Taking the boundary conditions expressed by equations (33) and (34) into consideration, equation (32) can be rewritten as equation (35).

$$\begin{aligned} & \int_{x_{surface}}^{x_{center}} D \times \frac{\partial F}{\partial x} \times \frac{\partial \omega}{\partial x} dx \\ & = F(x_{surface}, t) \times q_t - \int_{x_{surface}}^{x_{center}} F \times \frac{\partial \omega}{\partial x} dx \end{aligned} \quad (35)$$

Now, $\omega(x, t)$ is chosen for the arbitrary function $F(x, t)$. Equation (35) is rewritten as equation (36).

$$\begin{aligned} & \int_{x_{surface}}^{x_{center}} D \times \left(\frac{\partial \omega}{\partial x} \right)^2 dx \\ & = \omega(x_{surface}, t) \times q_t - \int_{x_{surface}}^{x_{center}} \omega \times \frac{\partial \omega}{\partial x} dx \end{aligned} \quad (36)$$

Furthermore, when $\omega(x, t)$ is expressed by the moisture content of each layer $\omega_1(t)$, $\omega_2(t)$, ..., $\omega_i(t)$, ... and $\omega_6(t)$, the moisture passing through the unit drying surface area per unit time q_t is expressed by equation (37).

$$q_t = \sum_{i=1}^6 \frac{d\omega_i(t)}{dt} \times l_i \quad (37)$$

Equation (36) can be rewritten as equation (38).

$$\begin{aligned} & \sum_{i=1}^6 D(\omega_i) \times \left(\frac{d\omega_i}{dx} \right)^2 \times l_i \\ & = \omega(x_{surface}, t) \sum_{i=1}^6 \frac{d\omega_i}{dt} \times l_i - \sum_{i=1}^6 \omega_i \times \frac{d\omega_i}{dt} \times l_i \end{aligned} \quad (38)$$

where, $d\omega_i/dx$ is the gradient of moisture distribution at the center $x=x_i$ of each layer. The position x_i which represents ω_i is as follows: $x_1=1.5$ mm, $x_2=4.5$ mm, $x_3=7.5$ mm, $x_4=10.5$ mm, $x_5=13.5$ mm and $x_6=16.5$ mm. If the diffusion coefficient is expressed by an exponential equation, that is,

$$D(\omega) = a \times e^{b(1-\omega)} \quad (39)$$

then, equation (38) can be rewritten as equation (40).

$$\begin{aligned} & a \sum_{i=1}^6 \left(e^{b(1-\omega_i)} \times \left(\frac{d\omega_i}{dx} \right)^2 \times l_i \right) \\ & = \omega(x_{surface}, t) \times \sum_{i=1}^6 \frac{d\omega_i}{dt} \times l_i - \sum_{i=1}^6 \omega_i \times \frac{d\omega_i}{dt} \times l_i \end{aligned} \quad (40)$$

Furthermore, as equation (40) must be satisfied at any drying time, equation (41) is derived.

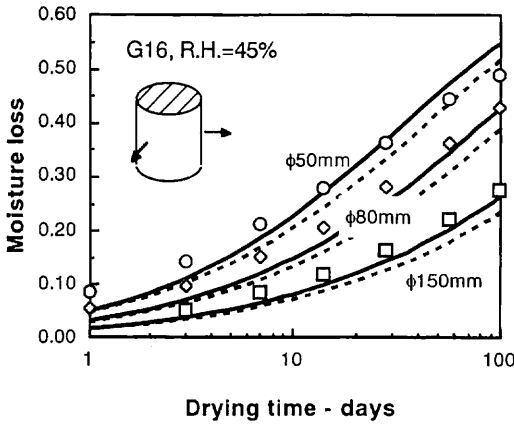


Fig.11 Moisture loss of cylinders with different diameter

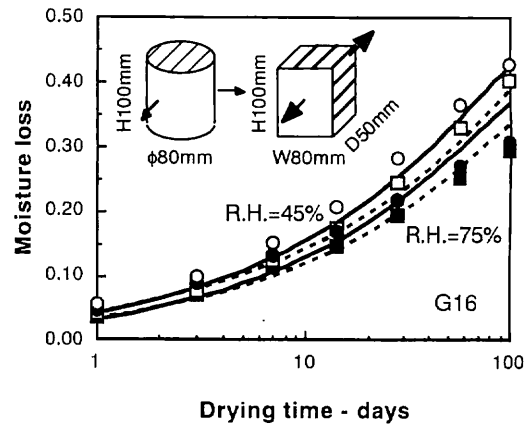


Fig.12 Moisture loss of (○) cylindrical and (□) prism specimens in 45% and 75% relative humidity

$$\begin{aligned}
 & a \sum_{i=0}^{i=98} \sum_{j=1}^6 e^{b(1-\omega_i)} \times \left(\frac{d\omega_i}{dx} \right)^2 \times l_i \\
 &= \sum_{i=0}^{i=98} \left(\omega(x_{surface}, t) \sum_{j=1}^6 \frac{d\omega_j}{dt} \times l_j - \sum_{j=1}^6 \omega_j \times \frac{d\omega_j}{dt} \times l_j \right) \quad (41)
 \end{aligned}$$

Now, $\omega(x_{surface}, t)$, $d\omega/dx$, and $d\omega/dt$ are known because the moisture distribution has been determined from the experimental data. Therefore, every factor in equation (41) except constants a and b is known. By using a least square method, constants a and b can be determined. The modified Marquart method is adopted in this study. The diffusion coefficients D_{sliced} and D_{solid} of concrete G16 in Table 1 are obtained by using the experimental results for sliced specimens and using the assumed moisture distributions of solid specimens calculated by equation (23), respectively.

$$D_{sliced} = 6.47e^{-3.23(1-\omega)} \quad (42)$$

$$D_{solid} = 9.15e^{-3.35(1-\omega)} \quad (43)$$

The smaller the diffusion coefficient, the slower the moisture loss. It is evident from a comparison of equation (42) and equation (43) that the diffusion coefficient of sliced specimens is smaller than that of solid specimens. It is obvious that the proposed numerical method precisely reflects the fact that moisture transfer in a pile of sliced specimen is slower than in a solid specimen.

3.4 Effect of air gaps on moisture transfer

Figure 11 shows the average moisture loss of three cylindrical specimens with different diameters for mix G16. Analogous specimens were made using the other mixes and similar results were obtained. The circles, lozenges, and squares are the experimental results obtained from cylinders with diameter 50, 80, and 150 mm, respectively. The height of these cylinders is 100, 100, and 150 mm, respectively. These results were obtained in the 45% relative humidity room. The top and the bottom surfaces were sealed with resin in order to prevent moisture transfer. Figure 12 shows the moisture loss of cylindrical and prism specimens measured in the 45% and 75% relative humidity rooms. Circles represent the experimental data for the cylinder. Squares are the experimental data for the prism. The data expressed by open marks and solid marks were measured in the 45% and 75% relative humidity rooms, respectively. The dimensions of cylindrical and prism specimens were $\phi 80 \times 100$ mm and $50 \times 80 \times 100$ mm, respectively. The top and bottom of the cylinder were sealed with resin. The four sides of the prism specimen were sealed with aluminum sheet. The drying surface was 80×100 mm. The curves were calculated by the finite element method. The

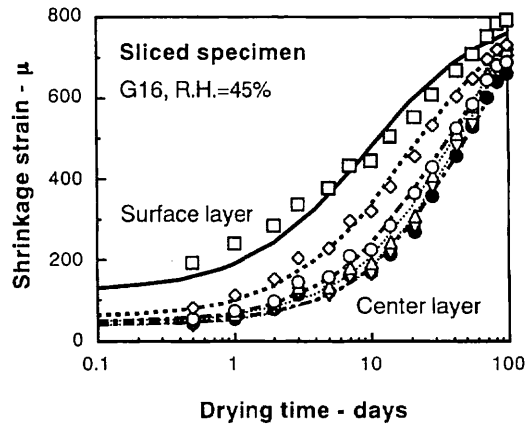


Fig.13 Shrinkage strain measured at each layer of a sliced specimen

broken line was calculated with the diffusion coefficient D_{sliced} as expressed by equation (42). The solid line was calculated with the diffusion coefficient D_{solid} as expressed by equation (43). It is clear from each figure that the difference between the calculated values with D_{sliced} and D_{solid} is very small and that the calculated curves fit the experimental data well. The effect of gaps between slices on the moisture transfer can be considered negligible.

4. RELATIVE HUMIDITY DISTRIBUTION

4.1 Relative humidity in mortar and concrete

Figure 13 shows the measured shrinkage strains of each layer of a pile of sliced specimen. Squares, lozenges, circles, triangles, inverted triangles, and solid circles are the data obtained from the drying surface layer, the second layer, and so forth to the center layer. The curves shown in this figure were obtained by regression analysis using equation (44).

$$Shrinkage\ strain = c_0 + \frac{c_2 \times t}{c_1 + t} \quad (44)$$

where, t is drying time; and c_0 , c_1 and c_2 are unknowns determined by the least square method. As the shrinkage strain of very thin specimens develops approximately linearly with changes in relative humidity, the relative humidity of the sliced specimen can be expressed using c_1 or c_0 and c_2 , as shown in equation (45).

$$\begin{aligned} Relative\ humidity\ of\ specimen &= 1 - \frac{(1 - R.H.) \times t}{c_1 + t} \\ &= 1 - (1 - R.H.) \times \frac{Shrinkage\ strain - c_0}{c_2} \end{aligned} \quad (45)$$

where $R.H.$ is the relative humidity in the surrounding atmosphere. Equation (45) indicates that the relative humidity of each thin slice of a specimen is 100% when drying time is equal to zero and that the relative humidity in specimen is equivalent to that of the atmosphere when the shrinkage strain reaches its ultimate value; that is, c_0 plus c_2 . The change in relative humidity of a specimen is expressed using the coefficient which expresses the development of shrinkage strain.

4.2 Diffusion coefficient as a function of relative humidity

Substituting the moisture content term ω in equation (41) by the relative humidity h_i term for cement-based materials, equation (41) may be rewritten as follows.

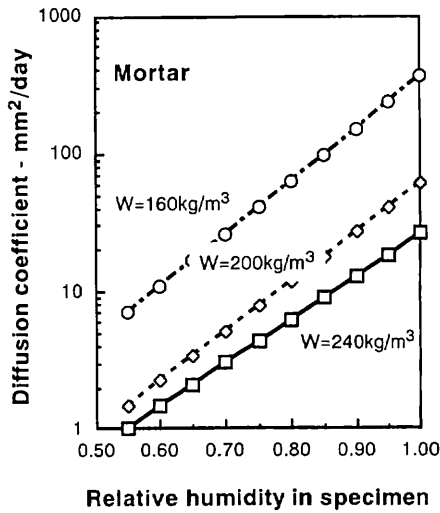


Fig.14 Diffusion coefficient of mortars M240, M200, and M160

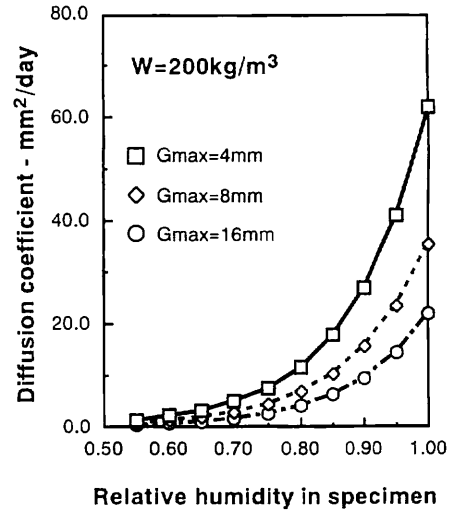


Fig.15 Diffusion coefficient of M200, G8, and G16

$$\begin{aligned}
 & a \sum_{i=0}^{t-98} \sum_{i=1}^6 e^{b(1-h_i)} \times \left(\frac{dh_i}{dx} \right)^2 \times l_i \\
 & = \sum_{i=0}^{t-98} \left(h(x_{surface}, t) \sum_{i=1}^6 \frac{dh_i}{dt} \times l_i - \sum_{i=1}^6 h_i \times \frac{dh_i}{dt} \times l_i \right) \quad (46)
 \end{aligned}$$

The diffusion coefficients of M240, M200, M160, G8, and G16 have been determined using equation (46). To obtain these diffusion coefficients, all measured data for the specimens for 45%, 60%, and 75% relative humidity were used. Results are given in equations (47) to (51).

$$M240: \quad D(h) = 26.3e^{-7.21(1-h)} \quad (47)$$

$$M200: \quad D(h) = 62.0e^{-8.29(1-h)} \quad (48)$$

$$M160: \quad D(h) = 36.3e^{-8.77(1-h)} \quad (49)$$

$$G8: \quad D(h) = 35.4e^{-8.15(1-h)} \quad (50)$$

$$G16: \quad D(h) = 22.0e^{-8.26(1-h)} \quad (51)$$

Figures 14 and 15 show the relationship between the diffusion coefficient and the relative humidity of mortar and concrete as expressed by equations (47) to (51). It is confirmed that the greater the maximum aggregate size, the smaller the diffusion coefficient. The results obtained by the proposed method are in agreement with the usual concept of moisture transfer in concrete due to drying.

4.3 Film coefficient

Figure 16 shows half the total relative humidity $Q/2$ of mortar M240 with respect to the drying time. The total relative humidity Q can be calculated with equation (52).

$$Q = \sum_{i=1}^{11} (1-h_i) \times l_i \quad (52)$$

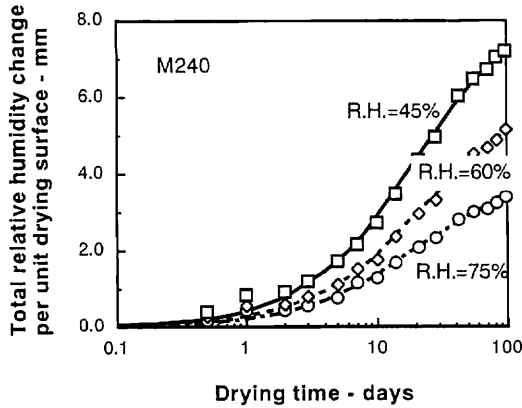


Fig.16 Total relative humidity change of M240

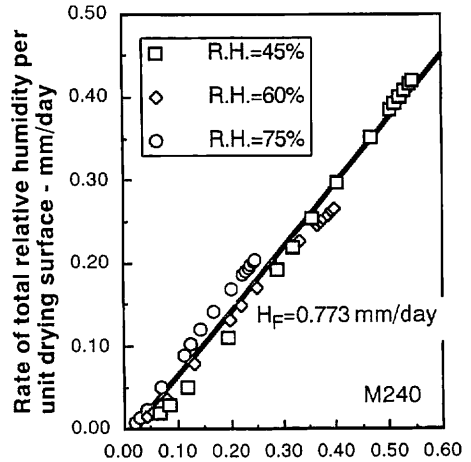


Fig.17 Film coefficient of M240

The film coefficient H_F expresses the relationship between q_t and $(h_{surface} - h_a)$ where q_t is the time differentiation of $Q/2$; $h_{surface}$ is the relative humidity on the drying surface; and h_a is the relative humidity of the surrounding atmosphere. The bigger the film coefficient, the more important the moisture transfer at the drying surface.

$$H_F = \frac{q_t}{h_{surface} - h_a} \quad (53)$$

$$q_t = \frac{1}{2} \times \frac{dQ}{dt} \quad (54)$$

Figure 17 shows the relationship between q_t and $(h_{surface} - h_a)$ in the case of M240. As is evident from this figure, the effect of the relative humidity of the surrounding atmosphere on the film coefficient is very small. Film coefficient H_F has been regressed using equation (53). For mixes M240, M200, M160, G8, and G16, the film coefficients are 0.773, 1.082, 2.502, 0.726, and 0.541 mm/day, respectively. It is confirmed that the bigger the maximum aggregate size, the smaller the film coefficient. Thus valid results for film coefficients are obtained, too.

4.4 Precision of the proposed method

Figure 18 compares the experimental data for relative humidity in each slice with the calculated values using the diffusion coefficient and the film coefficient described in the previous section. The curves in the figure are the calculated values, while the marks represent experimental data obtained from concrete G16 in the 45% relative humidity room. It is evident from this figure that the calculated values fit the experimental data very well.

5. DEFORMATION DUE TO DRYING

5.1 Shrinkage coefficient

The shrinkage coefficient expresses the change in strain as a function of moisture or relative humidity change. If a specimen is so thin that the moisture distribution can be regarded as constant, the shrinkage coefficient may be obtained directly. However, the deformation of a very thin specimen is strongly affected by carbonation, as shown in Figure 19. The shrinkage strain and weight change in this figure were measured on 100x150x3 mm prisms for 28

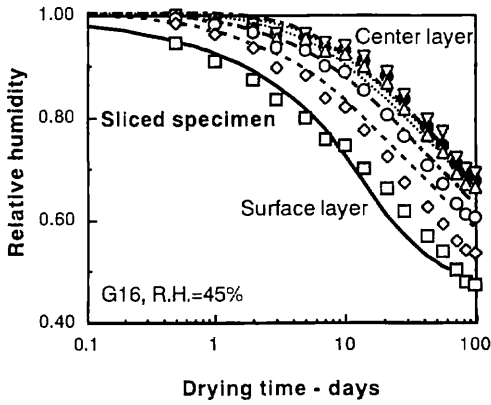


Fig.18 Comparison of calculated and experimental data for relative humidity as function of dring time

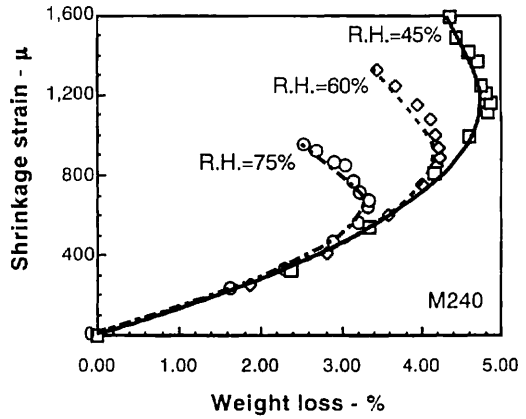


Fig.19 Shrinkage strain of very thin specimen

days. The horizontal axis is the weight change of the specimen divided by the weight before drying. This value is positive when moisture is lost. Within one week of drying, the weight of each specimen at all three levels of relative humidity increased, even though the specimens dried. This is the effect of carbonation. Hence it is impossible to determine the shrinkage coefficient of a very thin specimen except in the special case of a carbon dioxide free environment. A method of obtaining the shrinkage coefficient without the effect of carbon dioxide needs to be established [5].

Figure 20 shows the shrinkage strain measured for solid and sliced specimens. The deformation of sliced specimens due to drying increases almost proportionally to relative humidity change because each layer is unrestrained. On the other hand, the deformation of solid specimens is nearly independent of position due to eigenstresses which modify the deformation to ensure compatibility. It is clear that Bernoulli's hypothesis, which states that plane sections remain plane, holds for the drying deformation of solid specimens of this size. The stress condition of solid specimens can be expressed as follows.

$$\sigma_y = \sigma_z = f(x) \quad (55)$$

$$\sigma_x = \tau_{xy} = \tau_{yz} = \tau_{zx} = 0 \quad (56)$$

where x indicates position in the direction of thickness. As the shrinkage distribution $Sh(x)$ within a solid specimen changes along the x -axis, each strain is expressed as follows.

$$\varepsilon_y = \varepsilon_z = \frac{f(x)}{E}(1 - \nu) + Sh(x) \quad (57)$$

$$\varepsilon_x = -\frac{2\nu f(x)}{E} + Sh(x) \quad (58)$$

$$\gamma_{xy} = \gamma_{yz} = \gamma_{zx} = 0 \quad (59)$$

where, ν is the Poisson ratio and E is Young's modulus. Equation (60) is obtained by substituting equations (57), (58), and (59) into the condition of compatibility expressed by equations (61), (62), and (63).

$$\frac{d^2}{dx^2} \left\{ f + \frac{E}{1 - \nu} Sh(x) \right\} = 0 \quad (60)$$

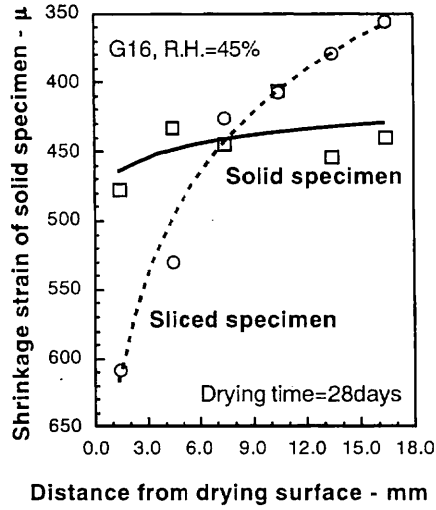


Fig.20 Shrinkage strain of piled sliced and solid specimens

$$\frac{\partial^2 \varepsilon_x}{\partial y^2} + \frac{\partial^2 \varepsilon_y}{\partial x^2} = \frac{\partial^2 \gamma_{xy}}{\partial x \partial y} \quad (61)$$

$$\frac{\partial^2 \varepsilon_y}{\partial z^2} + \frac{\partial^2 \varepsilon_z}{\partial y^2} = \frac{\partial^2 \gamma_{yz}}{\partial y \partial z} \quad (62)$$

$$\frac{\partial^2 \varepsilon_z}{\partial x^2} + \frac{\partial^2 \varepsilon_x}{\partial z^2} = \frac{\partial^2 \gamma_{zx}}{\partial z \partial x} \quad (63)$$

Equation (64), which expresses the stresses σ_y and σ_z , can be obtained by solving the differential equation (60).

$$\sigma_y = \sigma_z = f(x) = -\frac{E}{1-\nu} Sh(x) + C_1 + C_2 x \quad (64)$$

where C_1 and C_2 are constants. They are obtained under the condition that the resultant stress and moment at the edge of a specimen are equal to zero; that is,

$$\int_{-L}^{L'} \sigma_y dx = \int_{-L}^{L'} \sigma_z x dx = 0 \quad (65)$$

where $L'=16.5$ mm is half the thickness of a specimen. By using equation (65), constant C_1 and C_2 can be determined and equation (66) is obtained.

$$\begin{aligned} \sigma_y = \sigma_z \\ = \frac{E}{1-\nu} \left\{ -Sh(x) + \frac{1}{2L'} \int_{-L}^{L'} Sh(x) dx + \frac{3x}{2L'^3} \int_{-L}^{L'} Sh(x) x dx \right\} \end{aligned} \quad (66)$$

$$N_T = \int_{-L}^{L'} E \times Sh(x) dx \quad (67)$$

$$M_T = \int_{-L}^{L'} E \times Sh(x) \times x dx \quad (68)$$

If equations (67) and (68) are employed, equation (66) can be rewritten as equation (69). The stress distribution is

then expressed by equations (69) and (70).

$$\sigma_y = \sigma_z = \frac{1}{1-\nu} \left\{ -E \times Sh(x) + \frac{1}{2L'} N_T + \frac{3x}{2L'^3} M_T \right\} \quad (69)$$

$$\sigma_x = \tau_{xy} = \tau_{yz} = \tau_{zx} = 0 \quad (70)$$

The strain distribution can be expressed using equations (71), (72), and (73).

$$\varepsilon_y = \varepsilon_z = \frac{1}{E} \left\{ \frac{1}{2L'} N_T + \frac{3x}{2L'^3} M_T \right\} \quad (71)$$

$$\varepsilon_x = -\frac{2\nu}{(1-\nu)E} \left\{ \frac{1}{2L'} N_T + \frac{3x}{2L'^3} M_T \right\} + \left(\frac{1+\nu}{1-\nu} \right) \times Sh(x) \quad (72)$$

$$\gamma_{xy} = \gamma_{yz} = \gamma_{zx} = 0 \quad (73)$$

If Young's modulus at each position on the x -axis is the same, then N_T represented by equation (67) and M_T represented by equation (68) can be rewritten as follows.

$$N_T = l \times E \times (2Sh_1 + 2Sh_2 + 2Sh_3 + 2Sh_4 + 2Sh_5 + Sh_6) \quad (74)$$

$$M_T = 0 \quad (75)$$

where Sh_i is the shrinkage strain corresponding to the i -th layer with relative humidity change. Equations (74) and (75) take advantage of the symmetrical boundary condition. Equation (71) can be rewritten using equations (74) and (75) as follows.

$$\varepsilon_i(t) = \frac{l}{L} \times \sum_{i=1}^{11} Sh_i(t) \quad (76)$$

where $\varepsilon_i(t)$ is the shrinkage strain measured at position i in a solid specimen. As $l=3$ mm and $L=33$ mm, $l/L=1/11$. Equation (76) means that the deformation of this size of solid specimen due to drying is independent of measurement position.

If the solid specimen deformation shown in **Figure 20** did not include the effects of carbonation and creep due to eigenstresses, the relationship between shrinkage strain and specimen relative humidity could be expressed by equation (45). Otherwise, the relationship given in equation (45) could be used if the effects of carbonation and creep due to eigenstresses were also calculated and included in the deformation due to shrinkage. In reality, neither is the case.

When the relationship between shrinkage strain and relative humidity of a specimen is expressed by a power term to take into consideration the effects of carbonation and creep due to eigenstresses, equation (78) is derived.

$$Sh_i(t) = a \times (1 - h_i(t))^b \quad (77)$$

$$\varepsilon_{avg.}(t) = \frac{1}{11} \times a \sum_{i=1}^{11} (1 - h_i(t))^b \quad (78)$$

where, $\varepsilon_{avg.}(t)$ is the average deformation measured in a solid specimen.

$$\varepsilon_{avg.}(t) = \frac{1}{11} \sum_{i=1}^{11} \varepsilon_i(t) \quad (79)$$

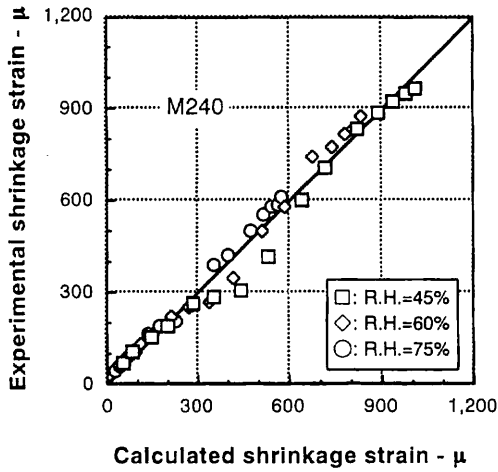


Fig.21 Precision of analysis results of M240

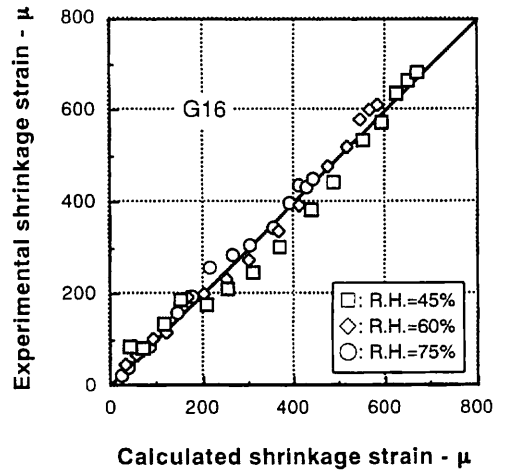


Fig.22 Precision of analysis results of G16

As equation (78) must be satisfied at any drying time, equation (80) can be derived:

$$\sum_{t=0}^{t=98} \varepsilon_{avg}(t) = \frac{1}{11} \times a \sum_{t=0}^{t=98} \sum_{i=1}^{11} (1 - h_i(t))^b \quad (80)$$

where, a and b are unknowns to be determined by the least square method. The relationship between shrinkage strain and relative humidity of M240, M200, M160, G8 and G16 obtained from equation (80) can be summarized by equations (81), (82), (83), (84), and (85), respectively. All data measured in the 45%, 60%, and 75% relative humidity rooms were used to obtain these equations.

$$\text{M240:} \quad Sh(h) = 2,17(1 - h(t))^{0.918} \quad (81)$$

$$\text{M200:} \quad Sh(h) = 1,84(1 - h(t))^{0.933} \quad (82)$$

$$\text{M160:} \quad Sh(h) = 1,53(1 - h(t))^{0.744} \quad (83)$$

$$\text{G8:} \quad Sh(h) = 1,32(1 - h(t))^{0.770} \quad (84)$$

$$\text{G16:} \quad Sh(h) = 1,37(1 - h(t))^{0.749} \quad (85)$$

It is confirmed that the higher the water content of the mortar, the greater the shrinkage strain, while the bigger the maximum aggregate size, the smaller the shrinkage strain. These results show that the experimental approach and numerical method proposed in this study give valid values.

5.2 Precision of the proposed method

Figures 21 and 22 compare the experimental shrinkage strains of solid specimens with the calculated values. The diffusion, film, and shrinkage coefficients obtained by the proposed method were used. Squares, lozenges, and circles represent data for the 45%, 60%, and 75% relative humidity cases, respectively. In both figures, the calculated data fit the experimental data well. It is found that the relationship between shrinkage strain and relative humidity expressed in equations (81) to (85) is adequate.

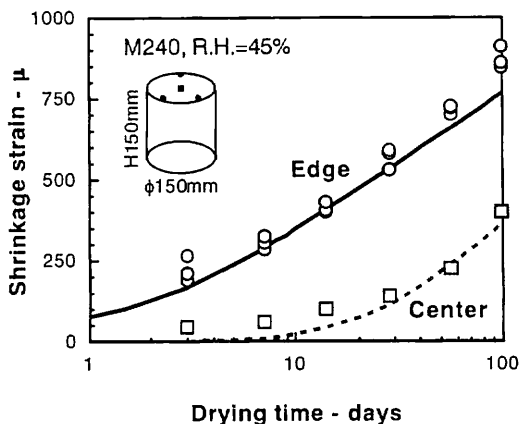


Fig.23 Shrinkage strain of cylinder specimen (M240)

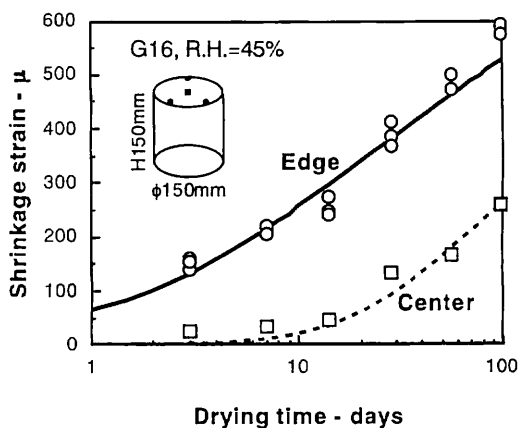


Fig.24 Shrinkage strain of cylinder specimen (G16)

6. VERIFICATION OF THE PROPOSED METHOD

Figures 23 and 24 show the deformation of cylinders due to drying for the M240 and G16 mixes (one cylinder only). The other mixes were also investigated and gave similar results. Circles and squares represent the experimental data measured at the center and the edge of the cylindrical specimens, respectively. The diameter and height of the specimens were both 150 mm. The top and bottom of the specimens were sealed with resin. These data were measured at 45% relative humidity. The curves in these figures were calculated by the finite element method using the diffusion, film, and shrinkage coefficients described in the previous sections. The results show that the calculated values fit the experimental data very well, and demonstrate the validity and applicability of the proposed method.

7. CONCLUSIONS

An experimental approach and a numerical method were proposed for obtaining the diffusion, film, and shrinkage coefficients of cement-based materials. The advantage of the proposed method is the direct determination of the diffusion coefficient as function of relative humidity for cement-based materials without the need for desorption isotherms. The results obtained from experiments with sliced specimens confirm that the influence of gaps between slices on the transfer of moisture can be neglected. Therefore, diffusion and film coefficients can be determined as functions of relative humidity using a pile of sliced specimens without the need to consider the effects of gaps. A new numerical method for obtaining diffusion coefficients from the moisture distribution or relative humidity distribution is proposed, based on the weighted residual method combined with a nonlinear least square method. The shrinkage coefficient was obtained from solid specimens. The thickness of the specimen satisfies Bernoulli's hypothesis. It was shown that the relationship between shrinkage strain and relative humidity of solid specimens can be expressed by a power law. Three mortars with different mix proportions and two concretes with aggregates of different maximum size were used. The diffusion, film, and shrinkage coefficients can be obtained for all types of cement-based materials. The results demonstrate the applicability of the method proposed in this contribution.

REFERENCES

- 1) Wittmann, F. H. : Grundlagen eines Modells zur Beschreibung charakteristischer Eigenschaften des Betons, Schriftenreihe Deutscher Ausschuss für Stahlbeton, Heft 290, Berlin, pp.43~101, 1977.
- 2) Wittmann, X., Sadouki, H. and Wittmann F. H. : Numerical Evaluation of Drying Test Data, Transactions 10th Int. Conf. on Struct. Mech. in Reactor Technology, SMiRT-10, Vol. R., pp.71~89, 1989.
- 3) Alvaredo, A. M., Helbling A. and Wittmann F. H. : Shrinkage Data of Drying Concrete, Building Materials Report No.4, Aedificatio Publishers, Freiburg, 1995.
- 4) Holm, A., Krus, M. und Künzel H. M. : Feuchttransport über Materialgrenzen im Mauerwerk, Internationale Zeitschrift für Bauinstandsetzen, Vol. 2, pp.375~396, 1996.
- 5) Alvaredo, A. M. : Drying Shrinkage and Crack Formation, Building Materials Report No.5, Aedificatio Publishers, Freiburg, 1994.